First radar measurements of ionospheric irregularities by the Radio Aurora Explorer CubeSat

Hasan Bahcivan[1], James Cutler[2], Matt Bennett[3], Ben Kempke[2], John Springman[2],
John Buonocore[1], Michael Nicolls[1], Rick Doe[1]

The Radio Aurora Explorer CubeSat detected the first radar echoes during the solar storm of 8 March 2012. The 300s ground-to-space bi-static radar experiment was conducted in conjunction with the Poker Flat Incoherent Scatter Radar in the local morning (8 am) over Poker Flat, Alaska. The geomagnetic conditions for the E-region field-aligned irregularity generation were optimal due to strong (greater than 1000 m/s) F-region ion drifts and sufficient E-region ionization (electron densities were ~1e11 m−3). The corresponding E-region electric field of > 50 mV/m was larger than the excitation threshold for the Farley-Buneman instability. Furthermore, an auto-correlation analysis showed the distribution of E-region backscatter with 3 km resolution in altitude and sub-degree resolution in aspect angle – unprecedented for auroral region measurements. Moreover, the measured Doppler of the UHF scatter shows the saturation speed of the meter-scale plasma waves. Raw data analysis is in progress to reveal fine angular structure of the FAI with respect to the geomagnetic field lines.

1. Introduction

Radio Aurora Explorer (RAX) is the first CubeSat funded by the NSF CubeSat-based Space Weather program. It is jointly conducted by SRI International and University of Michigan. The mission is a ground-to-space bi-static radar experiment designed to investigate the causes of upper atmospheric/ionospheric turbulence driven by solar wind and magnetospheric electromagnetic forcing. The plasma turbulence is composed of field-aligned irregularities (FAI) of electron density driven by various plasma instabilities.

Previously, FAI measurements have been obtained using ground-based coherent scatter radars. However, due to near vertical magnetic field line geometry at high-latitudes, it has been difficult to achieve scatter perpendicularity. The ground-based coherent scatter radar measurements made at very low elevation angles could not resolve the FAI in high spatial resolution and HF radars were subject to refraction resulting in source location ambiguity.

The unique radar scattering geometry of a RAX experiment, composed of a transmitter on the ground and an orbiting receiver in space, enables unique high-resolution measurements of FAI. Moreover, the RAX mission affords the opportunity to measure vector electric fields and plasma densities probed simultaneously by the incoherent scatter radar, enabling the establishment of a direct relationship between the FAI and the ionospheric drivers. The RAX mission science and radar system was described in detail in *Bahcivan et al.* [2009]; *Bahcivan and Cutler* [2012].

The RAX II satellite (shown in Figure 1) was launched on 28 October 2011 from Vandenberg Air Force Base to a 104° inclination, elliptical orbit (400–820 km). The launch was provided by NASA's Educational Launch of Nanosatellites (ELaNa) program. Following a successful spacecraft checkout, RAX II conducted the first experiment with the Poker Flat Incoherent Scatter Radar (PFISR) on 22 November 2011. Due to the snapshot nature of each experiment lasting only 300s and the probability of geophysical activity at a given time being low, a large number of experiments are needed to detect backscatter from FAI. For this reason, the mission lifetime was set at 1 year, assuming 1-2 experiment per week. So far, 18 experiments have been conducted. The results from the last experiment clearly show E-region radar backscatter.

Figure 1: *Experimental concept. Wave-driven currents induce an angular shift between radar estimates of ground magnetic deflections and actual magnetometer measurements*

2. Experiment description

Figure 2 shows the loci-of-perpendicularity for the satellite altitude of 800 km (the satellite was actually at the altitude of 811 km) and the satellite track shown by the dashed black line. The RAX radar receiver was turned on for 300s over the experimental zone, starting at 17:10:24 UT on 8 March 2012, collecting 14-bit I and Q samples at a rate of 1 MSPS each. The satellite track shown in this figure covers a duration of 170s, beginning at 75s and ending at 245s into the experiment. Since the GPS was turned off, the actual start time may be off by several seconds.

The blue cross in Figure 2 shows the location of PFISR on the ground. PFISR transmitted pulses in six beam directions. The beam dedicated to RAX reception was pointed at 20.8° east of north and at 58° elevation, sending 100ms uncoded pulses at 449 MHz every 10ms. The red cross shows the beam position at the spacecraft altitude. Halfway between the 100ms pulses for RAX, 480ms long pulses were transmitted to diagnose the background ionosphere using the incoherently scattered signals received back at PFISR. These pulses were transmitted at 449.5 MHz alternating between the 6 directions, one of which coincided with the direction of the 100ms pulse.

[1] SRI International, Menlo Park, CA, USA
[2] D. of Aerospace Engineering, U. Michigan, Ann Arbor, MI, USA
[3] Jet Propulsion Laboratory, NASA, Pasadena, CA, USA
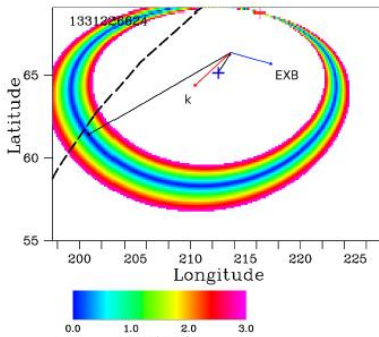
Figure 2: *Experimental geometry showing the loci of perpendicularity at the spacecraft altitude (colored rings), spacecraft trajectory (dashed line), the incoming and scattered radar wave direction (thin black line), and the scattering Bragg wavevector (red vector). Blue and red crosses mark the location of PFISR on the ground and the beam location at the spacecraft altitude, respectively. Finally, the blue vector shows the direction of the ExB drift during the pass.*
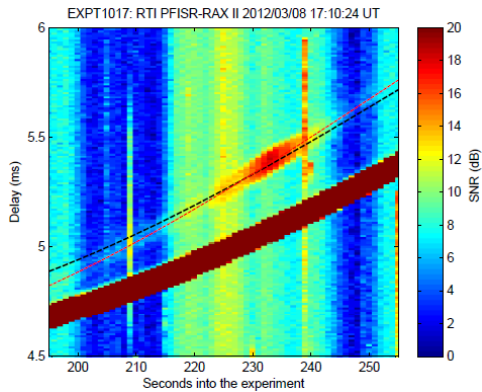
Figure 3: *Range-time-intensity plot for the duration of E-region echoes observed by RAX. The black line marks the arrival time of echoes from the altitude of 100 km. The red line is a visual fit to the trace of the echo peak.*

Every ten of the original RAX samples (collected at 100 MHz) were coherently averaged together resulting in a record length of 1000 samples per inter-pulse-period of 10ms. Then, the signal power was computed and 100 records were incoherent averaged to form a range-time-intensity profile for each second, as shown in Figure 3. Note that due to the variable amount of interference, no attempt was made to determine the noise floor. Instead, a preset noise power (computed based on lab measurements) was programmed into the on-board software. This noise floor was used to convert signal power to signal-to-noise ratio. After on-board computing that lasts ~1h, the 1.2 GB of raw I and Q data are finally converted to a post-compression 50 KB RTI image and downloaded.

In the several weeks following this experiment, the raw I and Q data corresponding to the 235th second (at the original 1 MHz rate) was also downloaded for Doppler analysis. The interference was carefully removed by matching a model signal to the interfering signal, which looked like Gaussian spikes lasting 7–8 ms and repeating at 10 KHz. These spikes were first removed and the missing data were interpolated using the adjacent samples. Note that the echo lasts about 140ms and appeared to have a correlation time in excess of 100ms, therefore, the effect of the interpolation in the analysis here is insignificant.

To measure the Doppler velocity of FAI, we computed the ACF lag at 90ms delay. This ACF was computed from 98 I and Q records corresponding to the 235th second (2 were manually excluded). We first computed the Doppler shift of the direct pulse from PFISR to RAX and applied a small frequency offset, df, to match to the Doppler shift corresponding to the projection velocity of the spacecraft along the PFISR line-of-sight, which was obtained from the ephemeris provided by North American Aerospace Defense command (NORAD). We then apply the same df to the Doppler shift of the I and Q samples containing the echo. Finally, we obtain the Doppler velocity of FAI by multiplying the corrected Doppler shift with the radar Bragg wavelength for the scattering geometry of the 235th second.

3. Observations

Figure 3 shows the RTI plot for this experiment. RAX crossed loci-of-perpendicularity for altitudes 300 (F region), 200, and 100 km (E region) at times approximately 175, 205 and 235 seconds into the experiment. Echoing occurred between the times 200–250s into the experiment. The echoes arrived 330ms after the arrival of the direct pulse, corresponding to E-region scattering altitudes. The strongest echoes occurred around 235s, corresponding to the altitude of 102 km. The peak SNR was 19 dB.

The black dashed-line in Figure 3 shows the expected location of the echoes originating from the altitude of 100 km. We notice that echoes arrive somewhat earlier on the left side of the plot and somewhat later on the right side. This is because altitudes lower (higher) than 100 km are contributing on the left (right) side.

The echo in Figure 3 was so well formed that we decided to fit a hyperbolic trace to it and determine the scattering geometry along the fitted trace (red dashed line). Figure 4 shows the SNR, aspect angle and altitude along the trace shown by the dashed red line in Figure 3. The peak of the SNR (red line) coincides remarkably well with the exact perpendicularity (green line) of the Bragg wavevector with the geomagnetic field. The altitude data (black line) shows that the peak SNR occurred at 102 km.

Figure 5 shows the echo power at 90ms ACF lag (red line) and the echo Doppler velocity (blue line) computed from the same lag (as discussed previously). The green line shows the power originally computed from the I and Q samples. Note that since the correlation time of UHF coherent scatter is on the order of 1ms [*Hall and Moorcroft*, 1988], the echo power computed from the ACF lag at 90ms is very well representative of the actual power. For the transmitted pulse of 100ms, the power from the ACF lag of 90 ms has a time resolution of 10ms, corresponding to an altitude resolution of 3 km.
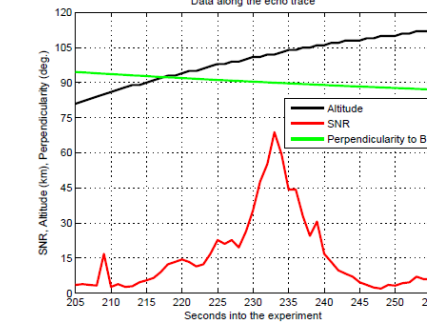
Figure 4: SNR (red line), aspect angle (green line), and altitude (black line) along the red trace shown in Figure 3.

4. Discussion

The literature on plasma waves in the auroral electrojet has been reviewed in *Haldoupis* [1989], *Sahr and Fejer* [1996], and *Moorcroft* [2002] among others. *Fejer et al.* [1975] solved for the frequency and growth rate of the waves with wavevector k:

$$\omega = \frac{\mathbf{k} \cdot (\mathbf{V}_{de} - \mathbf{V}_{di})}{1 + \psi} + \mathbf{k} \cdot \mathbf{V}_{di} \qquad (1)$$

$$\gamma = \frac{1}{1 + \psi} \left[\frac{\psi}{v_i} \left\{ (\omega - \mathbf{k} \cdot \mathbf{V}_{di})^2 - k^2 C_s^2 \right\} + \frac{k_\perp v_i}{k^2 L \Omega_i} (\omega - \mathbf{k} \cdot \mathbf{V}_{di}) \right] - 2\alpha n_o \qquad (2)$$

where

$$\psi = \frac{v_e v_i}{\Omega_e \Omega_i} \left(1 + \frac{\Omega_e^2}{v_e^2} \frac{k_\parallel^2}{k_\perp^2} \right). \qquad (3)$$

In the above equations, $\mathbf{V}_{de}$ and $\mathbf{V}_{di}$ are the electron and ion drift velocities, L is the transverse plasma density gradient scale length, α is the recombination coefficient, Ω and v_e refer to gyro and collision frequencies (with neutrals) for the ions and electrons, and Ψ is the so-called anisotropy factor, which depends on the magnetic aspect angle. The Cs term is the ion acoustic speed [*Farley*, 1963].

The above dispersion relation accounts for some of the properties of auroral E-region waves including (1) their excitation threshold, (2) their aspect sensitivity and (3) their Doppler spectrum.
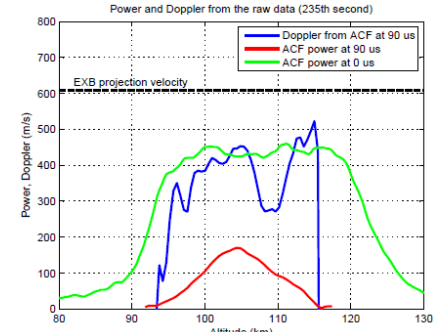
Figure 5: Raw echo intensity (green line), altitude-resolved intensity (red line) and Doppler velocity (blue line) as a function of altitude for the 235th second into the experiment (a vertical cut through the peak intensity in Figure 3).

First, the echoes are only observed when the line-of-sight electron drift speed exceeds a threshold speed close to Cs. For this experiment, the ion drift velocities measured by the Poker Flat Incoherent Scatter Radar during the 300s experiment had a magnitude of 1400 m/s, well exceeding the threshold (500 m/s) for the Farley-Buneman instability. The electron densities were around 2e11 m−3. The Poker Flat magnetometer recorded a horizontal component of ~550 nT, in line with large E-region electrical currents. Second, the radar echoes are highly aspect sensitive, with RMS aspect angles between 0.1° -0.4° [*Kudeki and Farley*, 1989]. Figure 4 clearly shows that the peak power coincides with the exact perpendicularity. Furthermore, the power fall of 10 dB occurs within 1–2°, in line with previous measurements at UHF (e.g., *Hall and Moorcroft* [1988]). Third, unlike the case of backscatter from the F region, auroral E-region coherent echoes do not exhibit Doppler shifts that are proportional to the line-of-sight convection speed in the scattering volume (see recent reviews by *Nielsen et al.* [2002]; *Uspensky et al.* [2003, 2004]). According to 30 MHz radar measurements reported in *Bahcivan et al.* [2005]; *Hysell et al.* [2008], the Doppler shift of the echoes are given by Cs*cosθ, where θ is the flow angle (between the radar Bragg wavevector and the main ExB flow direction) and the ion acoustic speed Cs is estimated according to the empirical formula derived from STARE-EISCAT measurements by *Nielsen and Schlegel* [1985].

The dashed horizontal line in Figure 5 shows the ExB drift projection velocity (~610 m/s) on the Bragg wavevector. The measured Doppler velocities of 300–400 m/s are lower than the dashed line, implying the saturation of the phase speeds. For this experiment the ExB drift was 1400 m/s. Furthermore, we see that the Doppler is increasing with altitude implying the increase of the ion acoustic velocity due to larger electron heating at higher altitudes (up to a certain height, ~115 km) [*Schlegel and St.-Maurice*, 1981; *St.-Maurice et al.*, 1981]. Finally, we observe a dip in the Doppler velocity which is indicative of a wind shear, similar to what was seen during the first Joule experiment.

5. Conclusion

Following a total of close to 18 ground-to-space radar experiments (end-to-end experiments, each of which resulted in a 300s range-time-intensity plot), the Radio Aurora Explorer CubeSat mission for the first time provided measurements of UHF auroral backscatter. The experiment coincided with the strong solar storm of 8 March 2012.

The work on raw data is in progress to characterize the aspect sensitivity of meter-scale waves with fine angular resolution.

Acknowledgements

Contact: Hasan Bahcivan (hasan.bahcivan@sri.com) for the references cited.